FRONTIERS OF BIOGEOGRAPHY
The scientific journal of The International Biogeography Society

Frontiers of Biogeography 18, 2025, e132274 | DOI 10.21425/fob.18.132274

RESEARCH ARTICLE

Timing and directionality of Triatominae (Hemiptera, Reduviidae) lineage dispersals in the Neotropics

Marina de la Barrera Cardozo[1], Jorge E. Rabinovich[2], Anderson Lepeco[3], Peter Löwenberg-Neto[4]

1 *Graduate Program in Neotropical Biodiversity, Universidade Federal da Integração Latino-Americana - UNILA, Foz do Iguaçu, Brazil*
2 *Center for Parasitological and Vector Studies, National Council for Scientific and Technical Research-La Plata Scientific and Technological Center, La Plata National University, La Plata, Argentina*
3 *Museu de Zoologia da Universidade de São Paulo, São Paulo, SP 04263-000, Brazil*
4 *Laboratório de Biogeografia, Universidade Federal da Integração Latino-Americana - UNILA, Foz do Iguaçu, Brazil*

Corresponding author: Peter Löwenberg-Neto (peter.lowenberg@unila.edu.br)

Editor Praveen Karanth
Received 16 July 2024 ♦ **Accepted** 27 June 2025 ♦ **Published** 15 July 2025

Abstract

Triatominae, commonly known as kissing bugs, are hematophagous insects of significant epidemiological concern due to their role as vectors for *Trypanosoma cruzi*, the causative agent of Chagas disease. Their widespread distribution across the Americas is a result of complex evolutionary and biogeographical processes. The objective of this research was to quantify the timing and directionality of Triatominae lineage dispersals throughout the New World. Using a time-calibrated phylogeny derived from genomic data and fossil evidence, anagenetic dispersals were modeled by the dispersal-extinction-cladogenesis (DEC) model followed by biogeographic stochastic mappings (BSM). Threshold regression analysis was employed to identify distinct dispersal phases and their predominant routes across 11 defined bioregions. Ancestral areas estimated by the DEC model indicated multiple areas as the ancestral range for the entire clade, with northern South America (BRG-18-19-20) identified as the most likely, albeit with small probability. A biphasic pattern in normalized dispersal rates was identified, characterized by two significant breakpoints at 50 Ma and 30 Ma, delineating three distinct phases. Phase A (60–50 Ma) showed high dispersal from the Amazonian region towards northern South America and Mesoamerica, potentially linked to warmer global temperatures. Phase B (50–30 Ma) exhibited a notable decline in dispersal activity, possibly influenced by global cooling. Phase C (30–0 Ma) marked a resurgence in dispersal, displaying complex and frequent patterns, including bidirectional exchanges between Mesoamerica and the Nearctic, and movements along the South American dry diagonal and along Atlantic bioregions. This comprehensive reconstruction provided novel insights into the anagenetic dispersal processes that shaped the historical and contemporary distribution of Triatominae species across the Americas.

Highlights

- A time-calibrated phylogeny places the origin of Triatominae at ~59.2 million years ago, indicating that the diversification of this subfamily may have occurred earlier than previously proposed in the literature.
- Analyses revealed a marked reduction in dispersal events among Triatominae lineages between 50 and 30 million years ago, coinciding with a phase of global cooling.
- Specific directional dispersal routes were reconstructed for each phase, revealing early Amazonian outflows and later complex bidirectional exchanges across the Americas.
- This comprehensive macroevolutionary reconstruction provided critical insights into the historical biogeography and current distribution patterns of Triatominae, vectors of Chagas disease.

Keywords

Dispersion-extinction-cladogenesis, dry diagonal, historical biogeography, Nearctic, Neotropical, niche conservatism, Rhodniini, South America, Triatomini

Copyright *Marina de la Barrera Cardozo et al.* This is an open access article distributed under the terms of the Creative Commons Attribution License (CC BY 4.0), which permits unrestricted use, distribution, and reproduction in any medium, provided the original author and source are credited.

Introduction

Commonly known as kissing bugs, Triatominae are hematophagous insects, primarily feeding on vertebrate blood (Galvão and Justi 2015), thus posing significant epidemiological concerns, as nearly all species serve as vectors for the protozoan *Trypanosoma cruzi*, Chagas, 1909, transmitting it to humans (Noireau and Dujardin 2010). These insects demonstrate remarkable versatility in their host selection, extracting blood from a variety of mammals, birds, amphibians, and reptiles (Rabinovich et al. 2011). Their feeding behaviors exhibit considerable mobility, driven by fluctuations on host abundance and vector population density (Minter 1976; Forattini et al. 1977; Gurtler et al. 2009).

Triatominae species thrive in a range of tropical, subtropical, and temperate environments (Galvão and Justi 2015), currently inhabiting a vast territory, spanning from the United States to Argentina in the Americas (Ceccarelli et al. 2022). While most Triatominae species are native to the Americas (Justi et al. 2016; Justi and Galvão 2017), a select few, including eight *Triatoma* Laporte, 1832 and six *Linshcosteus* Distant, 1904 species, are found in the Indomalayan, Australian (Monteiro et al. 2018), and African (Poinar-Jr 2019) realms. Originated in the Americas, the clade is believed to have dispersed to Asia through the Bering Strait between 25 and 10 million years ago (Ma) (Justi et al. 2016; Monteiro et al. 2018).

The Triatominae are included within the family Reduviidae (assassin bugs) and currently comprise 154 extant species and three fossils (Alevi et al. 2021; Weirauch 2021). American species of Triatominae display a latitudinal richness gradient, peaking further south of the equator (Rodriguero and Gorla 2004; Diniz-Filho et al. 2013; Fergnani et al. 2013), with their richness distribution pattern correlating positively with absolute temperature and inversely with temperature seasonality, particularly intensifying towards the eastern regions of South America (Rodriguero and Gorla 2004; Diniz-Filho et al. 2013; Fergnani et al. 2013). The underlying mechanism driving this pattern is likely related to the niche conservatism of regional assemblages, highlighting the intricate ecological dynamics shaping Triatominae distributions (Ibarra-Cerdeña et al. 2014; Ceccarelli et al. 2020).

The Triatominae subfamily originated from predatory reduviid bugs in the New World, with divergence estimates converging around 45–30 Ma during the Eocene or Oligocene (Monteiro et al. 2018), although earlier molecular dating suggested a much older divergence, 107–64 Ma (Weirauch 2021). This group most likely originated in Central or northern South America (Justi et al. 2016), their diversification was profoundly shaped by major geological events, including the Andean uplift and the formation of the Pebas system (23–10 Ma), which influenced the spread of groups like the Rhodniini and Triatomini across the Neotropics (Abad-Franch and Monteiro 2007; Justi et al. 2016). Dispersal routes were diverse, with ancestors of Old World Triatominae reaching Eurasia via the Bering Land Bridge around 20 Ma, and colonizations of the Antilles occurring from ~34 Ma via land bridges and later by hitchhiking (Justi et al. 2016; Monteiro et al. 2018). Within South America, lineages like *Panstrongylus* secondarily occupied Amazonian ecoregions after the Panama Isthmus closure (~3 Ma), while others, such as *Triatoma maculata*, represent ancient relicts of dry forest corridors, illustrating a complex history of vicariance and dispersal that continues to define their global distribution (Abad-Franch and Monteiro 2007). Additionally, the dispersal of Triatominae lineages has likely played a significant role in determining the species' current distribution, particularly over the past 10 million years (Justi et al. 2016).

The historical trajectory of the Rhodniini tribe originated approximately 17.91 million years ago, diverging from specialist termite predators around 30.43 Ma (Paula et al. 2021). Their evolutionary path is largely characterized by vicariance events, with the oldest extant species, *Rhodnius domesticus* Neiva & Pinto, 1923, emerging 9.13 Ma. Major geological transformations, such as the formation of the Pebas system (23–10 Ma) and the uplift of the Andes, drove the allopatric speciation of key clades, including the trans-Andean *pallescens* and cis-Andean *pictipes* groups. Subsequent hydrological connections and the expansion of arid biomes further shaped the distinct bioclimatic niches and dispersal routes of species across the Neotropics (Paula et al. 2021).

The evolutionary trajectory of *Triatoma infestans* (Klug, 1834) originated in the Bolivian highlands less than 2.7–1.0 million years ago. Its widespread distribution across the Americas is largely attributed to a recent adaptation to human dwellings, driving two major dispersal waves: an initial, earlier spread through the Andean regions of Bolivia and Peru (potentially pre-Incaic/Incaic), and a more extensive, rapid expansion into the non-Andean lowlands of Chile, Paraguay, Argentina, Uruguay, and Brazil (primarily post-Columbian), profoundly shaped by human migration and settlement (Bargues et al. 2006).

Lineage dispersal, characterized by the anagenetic establishment of an evolutionary lineage in a new area while also remaining in the source area (Ree et al. 2005; Ree and Smith 2008), represents a fundamental process alongside speciation and extinction in the formation of taxonomic assemblages over time (Antonelli et al. 2018; Löwenberg-Neto and de Carvalho 2020; Löwenberg-Neto 2024). The primary objective of this research was to quantify the timing and directionality of Triatominae lineage dispersals throughout the New World, to understand how major geological and climatic events have shaped their evolutionary trajectory and present-day geographic patterns. Additionally, we aim to shed light on the role of lineage dispersal in shaping the current distribution of Triatominae species across the Neotropics, contributing to the understanding of the macroevolutionary processes underlying the emergence and spread of this medically important insect group.

Methods

Phylogenetic tree

Phylogenetic relationships were based on results provided by Kieran et al. (2021), which includes a comprehensive sampling of Triatominae species. The topology used is the maximum likelihood tree resulting from analysis of over 2,500 ultraconserved elements (UCEs) and three ribosomal markers, with UCEs filtered to a matrix of 85% completeness and partitioned by loci (fig. 3 in Kieran et al. 2021). Tree inference was conducted in RAxML v8.1.20 (Stamatakis 2014) and the resulting tree was rooted using *Lisarda inornata* as outgroup (Walker 1873), following recent phylogenomic results (Zhang et al. 2016; Knyshov et al. 2023; Masonick et al. 2025).

For generating a time-calibrated tree, we used the complete tree retrieved by Kieran et al. (2021) as input in MD-Cat (Mai et al. 2024). This recently proposed method takes as input a single tree with calculated branch-lengths altogether with a list of calibrations in geological time. Applying a categorical rate model and the Expectation-Maximization algorithm, MD-Cat provides an ultra-fast approach for phylogenomic dating, providing results congruent with those generated by most widespread algorithms (Mai et al. 2024). An age of 84 Ma was assumed for the root, following the estimates recovered for the most recent common ancestor of *Lisarda inornata*, *Pasiropsis* sp., and Triatominae *sensu* Masonick et al. (2025) by Hwang and Weirauch (2012).

Two additional calibration points were defined based on fossil information. The first corresponds to the Dominican amber species *Triatoma dominicana* Poinar Jr., 2005. Following Weirauch and Hwang (2012), this fossil was used as information for calibrating the most recent common ancestor of the less inclusive clade including *Triatoma protractra* Uhler 1894 + *Paratriatoma hirsuta* Barber, 1938 + *T. dimidiata* (Latreille, 1811) + *T. recurva* (Stål, 1868). An age of 17.1 Ma was attributed to this node, representing the mean age estimated for Dominican amber (www.paleobiodb.org, see also Iturralde-Vinent and MacPhee 2019). A second calibration point with the same age was defined based on *Panstrongylus hispaniolae* Poinar Jr. 2013, also from Dominican amber. This fossil species has been considered as similar to the extant *Panstrongylus geniculatus* (Latreille, 1811) and was used to calibrate the clade uniting this species and *P. chinai* (Del Ponte, 1929).

We ran an MD-Cat analysis using the -b flag which calculates ages in backward time, using 50 rate categories. The optimization of ages was performed 200 times from different initial states before results were drawn (-p = 200). Sequence length was set to 85,293 bp, which was the total length of the alignment used by Kieran et al. (2021) for inferring the original tree (-l = 85293). Other parameters were set as default. The resulting tree was then used as input in R program v.4.4.3 for visualization and removal of outgroup taxa. In this case, we used the definition of Triatominae of Kieran et al. (2021) and excluded taxa of the tribes Opisthacidiini, Zelurini, and Zeluroidini (see Masonick et al. 2025). In addition, we pruned the tree to include only taxa with available distributional information.

Species occurrences

Our geographic dataset comprised occurrence records primarily from the DataTri database (Ceccarelli et al. 2022), a comprehensive and curated source of Triatominae distribution data. For six species absent from DataTri—*Linshcosteus karupus*, *Linshcosteus costalis*, *Triatoma bouvieri*, *Triatoma brailovsky*, *Triatoma obscura* and *Triatoma cavernicola*—we obtained occurrence points from original taxonomic descriptions and published records (Ghauri 1976; Else et al. 1977; Galvão et al. 2002; Leite 2013; Kieran et al. 2021). After consolidating all occurrence records and eliminating duplicates, we compiled a dataset of 18,438 unique geographic points across the 103 Triatominae species considered. Species lacking any occurrence within the studied area were excluded, resulting in a final set of 96 species.

Regionalization scheme

The geographic dataset of occurrence points was mapped and geocoded into a multiple-area range scheme (Hackel and Sanmartín 2021). For this analysis, we adopted area ranges identified for the American Triatominae species distributions based on the network approach (Ferrari et al. 2022). To delineate these areas, Ferrari et al. (2022) implemented Infomap Bioregions, an approach that employs an adaptive resolution framework, adjusting cell sizes in response to the spatial density of species distribution data. A bipartite network of cells and species was constructed, simplified through the Map Equation algorithm, and clustered into bioregions using Markov chains (Edler et al. 2016). Then, to compare results from Bioregions analyses, they employed a metaconsensus criterion using UPGMA (unweighted pair-group method with arithmetic averages) based on Bsim dissimilarity. This analysis revealed hierarchical relationships among 23 bioregions. To meet our computational limitations, we reduced the number of areas to a set of 11 bioregions. This reduction was based on the UPGMA dendrogram structure (Ferrari et al. 2022), where bioregions exhibiting species composition similarity were grouped together. BRG 7 was omitted from our modified scheme because it spatially coincided with BRG-3, 5, 6, 8, 9, 10, and 11. The bioregion code used here represents the grouping of the original bioregions. To avoid overestimating species ranges, we manually reviewed and removed isolated points located at bioregional boundaries when the species was otherwise widely distributed in adjacent areas. Based on this spatial assessment, we generated a binary presence/absence matrix (Suppl. material 1: table S1).

Lineage dispersal modelling

We fitted the presence/absence matrix and the phylogenetic tree to a dispersal-extinction-cladogenesis (DEC) model — a continuous-time model for geographic range evolution that estimates ancestral ranges within a likelihood framework while modeling two free parameters along the branches: dispersal and extinction (Ree et al. 2005; Ree and Smith 2008; Ree and Sanmartín 2018). In the context of the DEC model, the term "dispersal" refers to the anagenetic establishment of an evolutionary lineage in a sink (new) area while maintaining its range in the source area (Ree et al. 2005; Ree and Smith 2008). We implemented the DEC model using the R package 'BioGeoBEARS' v.1.1.3 (Matzke 2018) with a maximum ancestral range of eight areas, as this was the highest number observed in the analyzed data. Dispersal was allowed without restriction between all areas in the model setup. Subsequently, we simulated the dispersal parameter by applying biogeographic stochastic mapping (BSM) (Hackel and Sanmartín 2021). BSM is a simulation approach that, based on the maximum likelihood estimates of dispersal and extinction, provides possible histories of changes along branches and avoids overestimating confidence in a single reconstruction (Dupin et al. 2017). We simulated 100 stochastic mappings to deal with age uncertainties (Magalhaes et al. 2021), presenting the results as event counts, averages, and frequencies across these mappings.

Timing, dispersal phases and directionality

For the timing analysis, we constructed histograms with 1-million-year bins to display the frequency of events across the 100 mappings. Because the number of branches in the phylogeny increases over time—leading to an inherent rise in the raw count of dispersal events (Antonelli et al. 2015)—we normalized these counts by the number of lineages through time (Löwenberg-Neto and de Carvalho 2020; Löwenberg-Neto 2024). This analysis was performed using the 'ape' package in R (Paradis and Schliep 2019), which also enabled us to generate a lineage-through-time plot.

To evaluate the temporal trend of the normalized dispersal rate, we employed the Sieve-bootstrap Student's t-test from the 'funtimes' package in R (Noguchi et al. 2011), revealing a nonlinear pattern. Consequently, we applied LOESS smoothing to fit a local regression model (Dornelas et al. 2013). Then, we fitted a threshold regression model to identify the number and the location of changing points, R package 'strucchange' (Zeileis et al. 2002). We constructed models between zero and six breaking points and we compared them by pairs, by the command 'anova()', to identify the best-fit model for the data. Assessing deviations from stability within a regression model facilitates the identification of distinct time periods characterized by varying linear trend dynamics. This analytical approach is particularly advantageous in time series analyses, as it enables the detection of phase shifts and the precise estimation of optimal breakpoint locations (Dornelas et al. 2013). Intervals between identified breakpoints were defined as dispersal phases.

Dispersal phases were adopted as a temporal framework for describing route directionality. We visualized the most frequent routes using a network representation with the arrows indicating the direction of the dispersal routes (Antonelli et al. 2018; Löwenberg-Neto and de Carvalho 2020). As an exploratory approach, we plotted dispersal phases onto the global surface paleotemperature record (Hansen et al. 2013; Tierney et al. 2020) and subjected to statistical comparison. Data normality was assessed using the Shapiro–Wilk and Anderson–Darling tests, and homogeneity of variances was evaluated via Levene's test. As the assumptions for parametric analysis were not fully satisfied, we applied the Kruskal–Wallis non-parametric test to compare phases, followed by Dunn's post hoc test to identify significant pairwise differences.

Results

The final tree including estimates of divergence times included 103 species of Triatominae (Fig. 1). MD-Cat analysis retrieved an age of 70.6 Ma for Triatominae *sensu* Masonick et al. (2025) and of 59.2 Ma for the most recent common ancestor of the tribes Triatomini, Cavernicolini, and Rhodniini (Triatominae *sensu* Kieran et al. 2021).

The modified Triatominae regionalization scheme comprised 11 bioregions. The analysis of species' geographic ranges against the regionalization scheme revealed that 52 species (54%) were found exclusively within a single bioregion, and 25 species (26%) occurred in two bioregions. The richest bioregion in number of species was BRG-18-19-20, and five bioregions showed 20 or more species (Suppl. material 1: fig. S1).

Ancestral areas were estimated by the DEC model and multiple areas were estimated as the ancestral area for the entire clade (Suppl. material 1: fig. S2). The simplified reconstruction showed that the most likely ancestral area, although with a small probability, was BRG-18-19-20, covering parts of northern South America and Mesoamerica (Fig. 2). Biogeographic stochastic mapping replicates of the dispersal parameter (d) resulted in 6,591 dispersal events. The temporal trends indicated that dispersal events were infrequent between 60 and 20 million years ago and gradually increased over time starting around 20 million years ago. This incremental trend culminated in a pronounced surge from 10 million years ago to the present day (Fig. 3A).

Although the absolute frequency increased toward the present, the frequency normalized by the number of lineages demonstrated a distinct trend. The normalized raw data exhibited periodic fluctuations that could be interpreted as alternating bursts of high and low dispersal activity; however, the smoothed trend line more accurately encapsulated a biphasic pattern. It was best described as an initial, pronounced decline from approximately 60 to 35 million years ago, followed by a gradual recuperation toward the present (Fig. 3C).

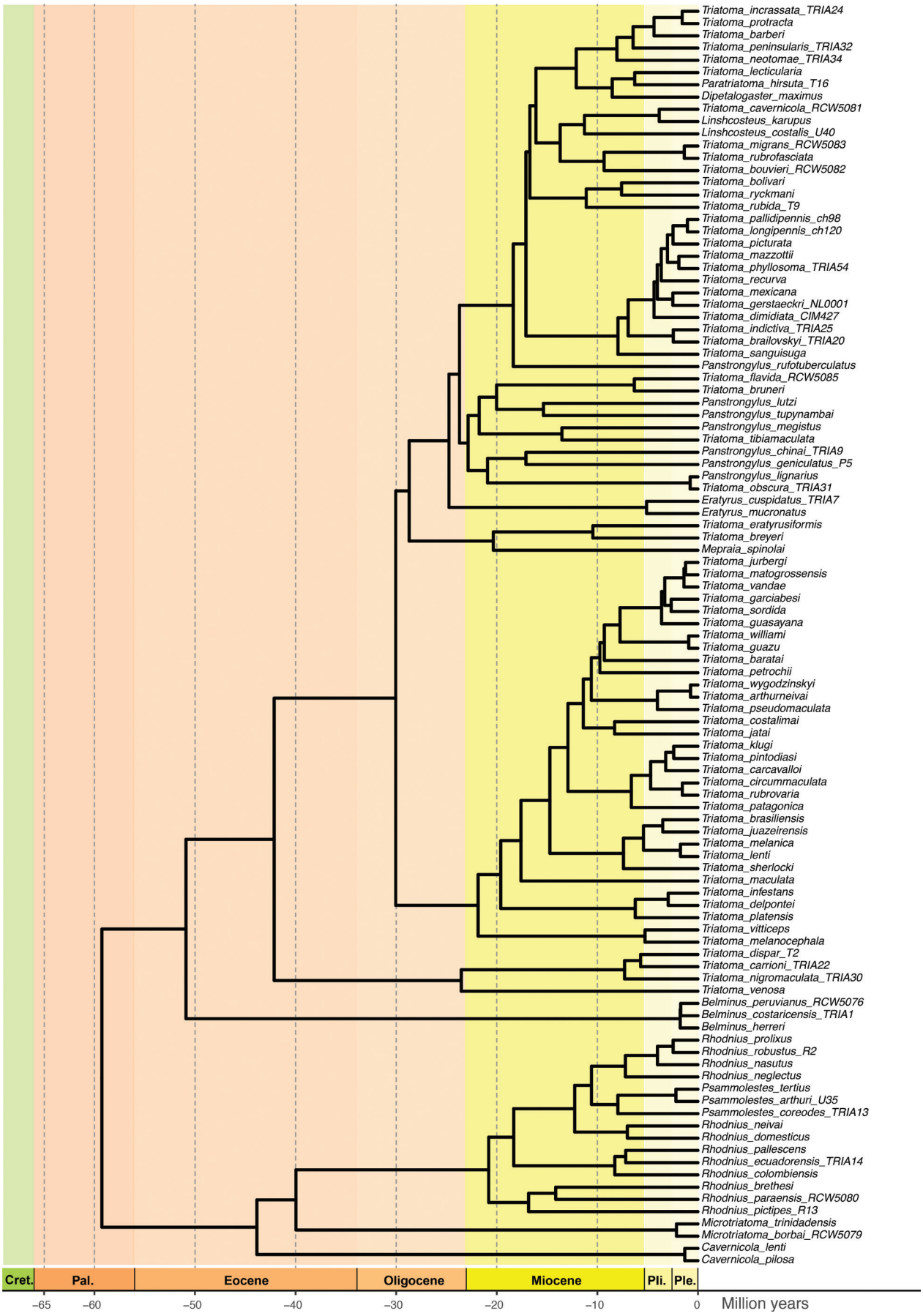

Figure 1. Triatominae time-calibrated phylogeny (modified from Kieran et al. 2021) generated on RAxML and MD-Cat with two calibration points from Dominican amber. Triatominae terminals were restricted to those with geographic occurrence data. Outgroup taxa were omitted.

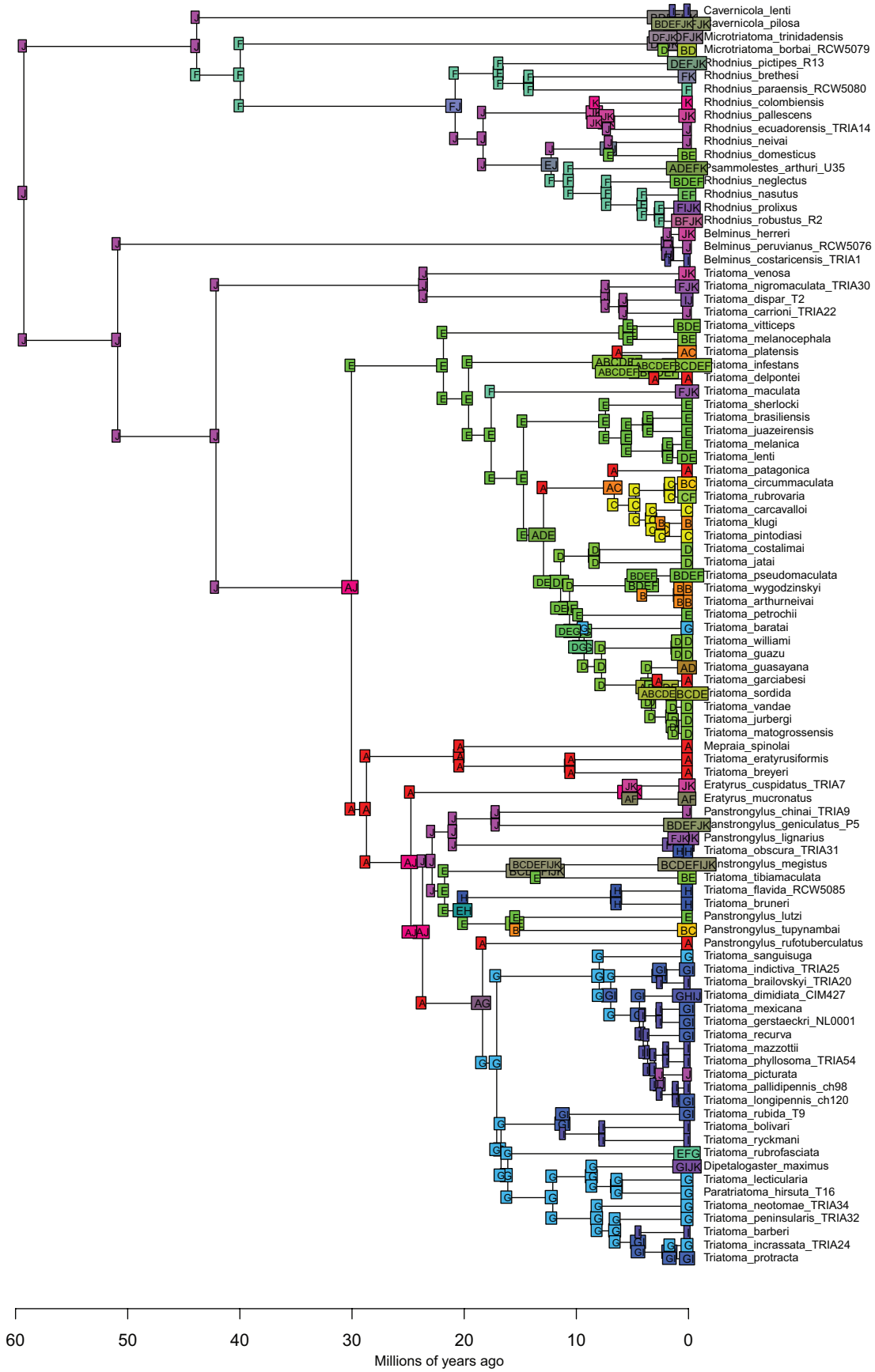

Figure 2. Triatominae ancestor areas estimated by the DEC model (8 areas max. d = 0.0069; e = 0.0026; LnL = -413.41). Rectangles depict ancestral ranges and letters depict terminal geographic ranges: A = BRG-1-2; B = BRG-3; C = BRG-4; D = BRG-5-6; E = BRG-8-9-10-11; F = BRG-12; G = BRG-13-14; H = BRG-15; I = BRG-16-17; J = BRG-18-19-20 ; K = BRG-21-22-23.

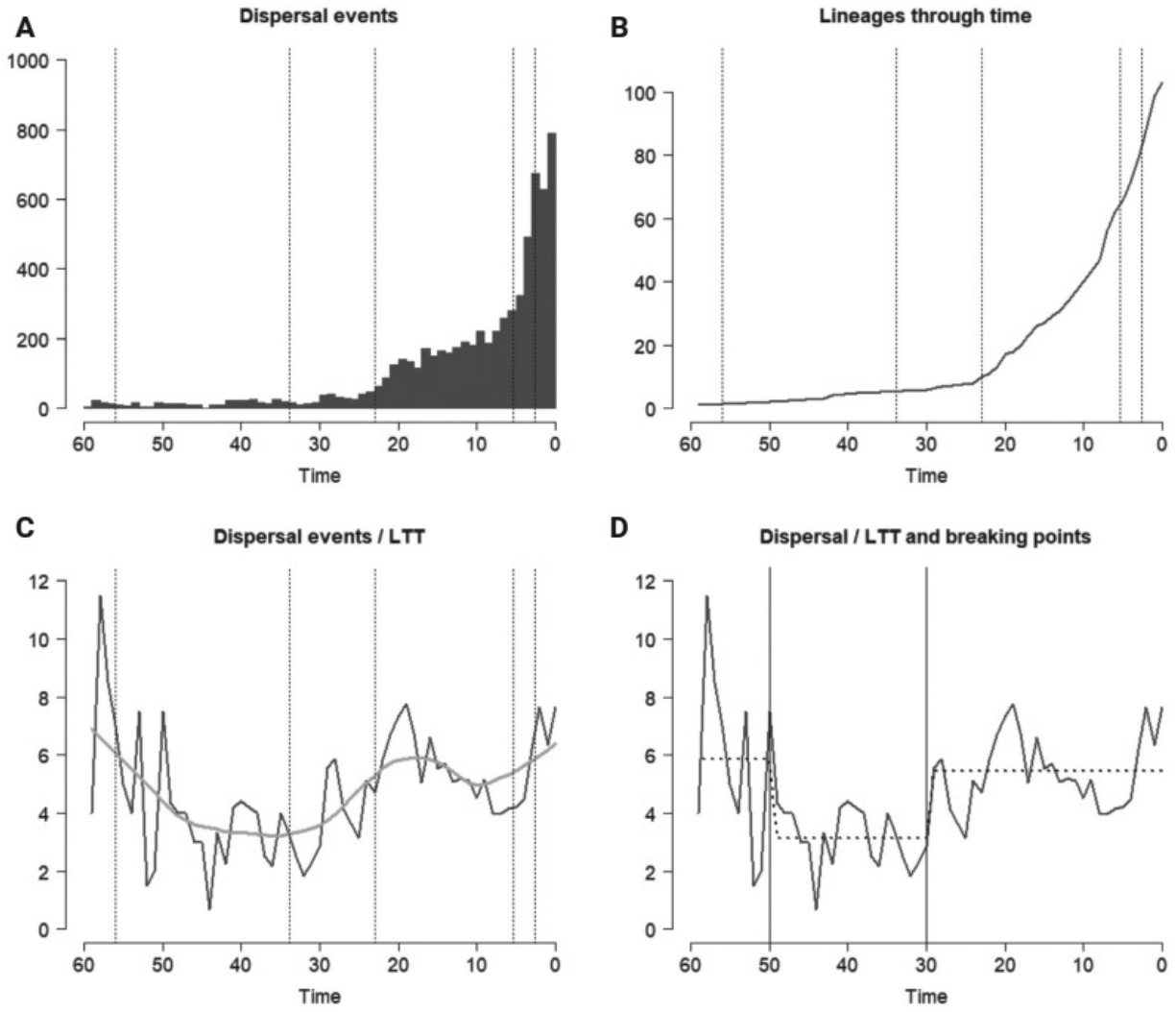

Figure 3. Timing of the Triatominae lineage dispersals in millions of years before the present. **A.** Frequency of dispersal events through time across 100 BSMs. **B.** Number of lineages through time in millions of years before the present. **C.** Rate of dispersal events through time, which is the number of events per number of lineages in 1-million-year bins; loess smoothing curve (continuous grey line). **D.** Rate of dispersal events through time and two breaking points (50 and 30 Ma, vertical solid lines), delimiting time periods with different linear trends (preferred model of threshold regression, dash-dotted line). Vertical dotted lines in **A, B** and **C** depict boundaries of stratigraphic epochs: 56.0 Ma, Paleocene-Eocene; 33.9 Ma, Eocene-Oligocene; 23.03 Ma, Oligocene-Miocene; 5.333 Ma, Miocene-Pliocene; and 2.58 Ma, Pliocene-Pleistocene.

The threshold regression model revealed significant phase shifts and corroborated the biphasic pattern. The best-fit model showed two breakpoints, 50 and 30 Ma, delineating three distinct time periods. The period between 60 and 50 million years ago (phase A) was followed by a substantial decline and stabilization during the 50–30 million years interval (phase B), indicating a phase of reduced dispersal dynamics. Then, in the most recent interval, from 30 million years ago to the present (phase C), a gradual resurgence in dispersal activity was observed (Fig. 3D).

The directionality of the most frequently observed dispersal routes was mapped for each dispersal phase (Figs 4, 5, 6). During phase A (60–50 Ma), lineages dispersed from the Amazonian region (BRG-12) toward northern South America (BRG-18-19-20) and from northern South America (BRG-18-19-20) towards Mesoamerica (BRG-16-17), as well as from the Caatinga (BRG-8-9-10-11) toward the Cerrado (BRG-5-6, Fig. 4). In phase B (50–30 Ma), dispersal occurred among Mesoamerica (BRG-16-17) and northern South America (BRG-18-19-20) and from northern South America (BRG-18-19-20) towards the Páramos (BRG-21-22-23), Caatinga (BRG-8-9-10-11), and Chaco (BRG-1-2). Additionally, routes from the Páramos (BRG-21-22-23) towards the Amazonia (BRG-12) and from the Amazonia (BRG-12) towards northern South America (BRG-18-19-20) were documented (Fig. 5). In phase C (30–0 Ma), a high frequency of bidirectional dispersals was observed between Mesoamerica (BRG-16-17) and the Nearctic region (BRG-13-14). Dispersal events also took place among Mesoamerica (BRG-16-17) and northern South America (BRG-18-19-20) bioregions. From the Amazonian bioregion (BRG-12), routes extended towards the Páramos (BRG-21-22-23)

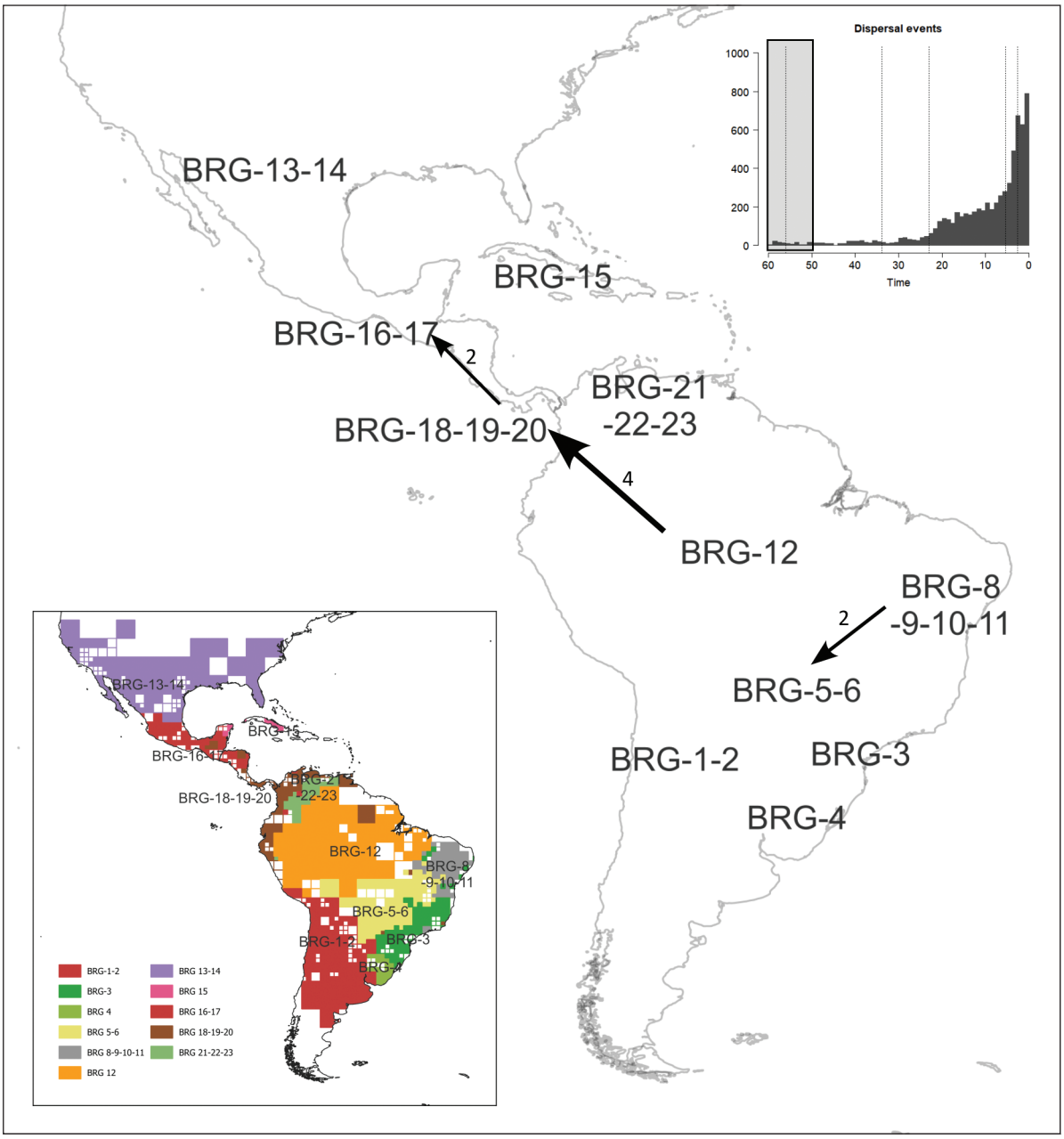

Figure 4. Most frequent dispersal routes of Triatominae between 60 and 50 Ma (phase A). Arrows represent the direction, and line thickness represents the frequency of dispersal events. The bioregion code used here represents the grouping of the original bioregions (Ferrari et al. 2022), for instance BRG-1-2 = BRG-1 + BRG-2.

and the Caatinga (BRG-8-9-10-11). Within the Atlantic biomes, there was a dynamic and reciprocal exchange between the Caatinga (BRG-8-9-10-11) and the Atlantic Forest (BRG-3). Further, dispersal routes were identified from the Caatinga (BRG-8-9-10-11) to the Cerrado (BRG-5-6), from the Cerrado (BRG-5-6) to the Chaco (BRG-1-2), and from the Chaco (BRG-1-2) to the Pampas (BRG-4), all following the South American dry diagonal. From the Pampas (BRG-4), dispersal routes were observed toward both the Atlantic Forest (BRG-3) and the Amazon Forest (BRG-12, Fig. 6). The timing of the twelve topmost frequent dispersal routes were plotted in histograms (Suppl. material 1: fig. S3) and descriptive statistics (Suppl. material 1: table S2).

A comparative and exploratory visualization of dispersal phases alongside the global surface paleotemperature record was presented (Fig. 7A). Non-parametric test revealed significant differences across the dispersal phases, and post hoc test pinpointed that they significantly differed among each other (Fig. 7B).

Discussion

While previous studies have explored aspects of the distribution and evolutionary history of the Triatominae (e.g. Justi et al. 2016), no study to date has provided a comprehensive analysis integrating phylogenetic timing, and

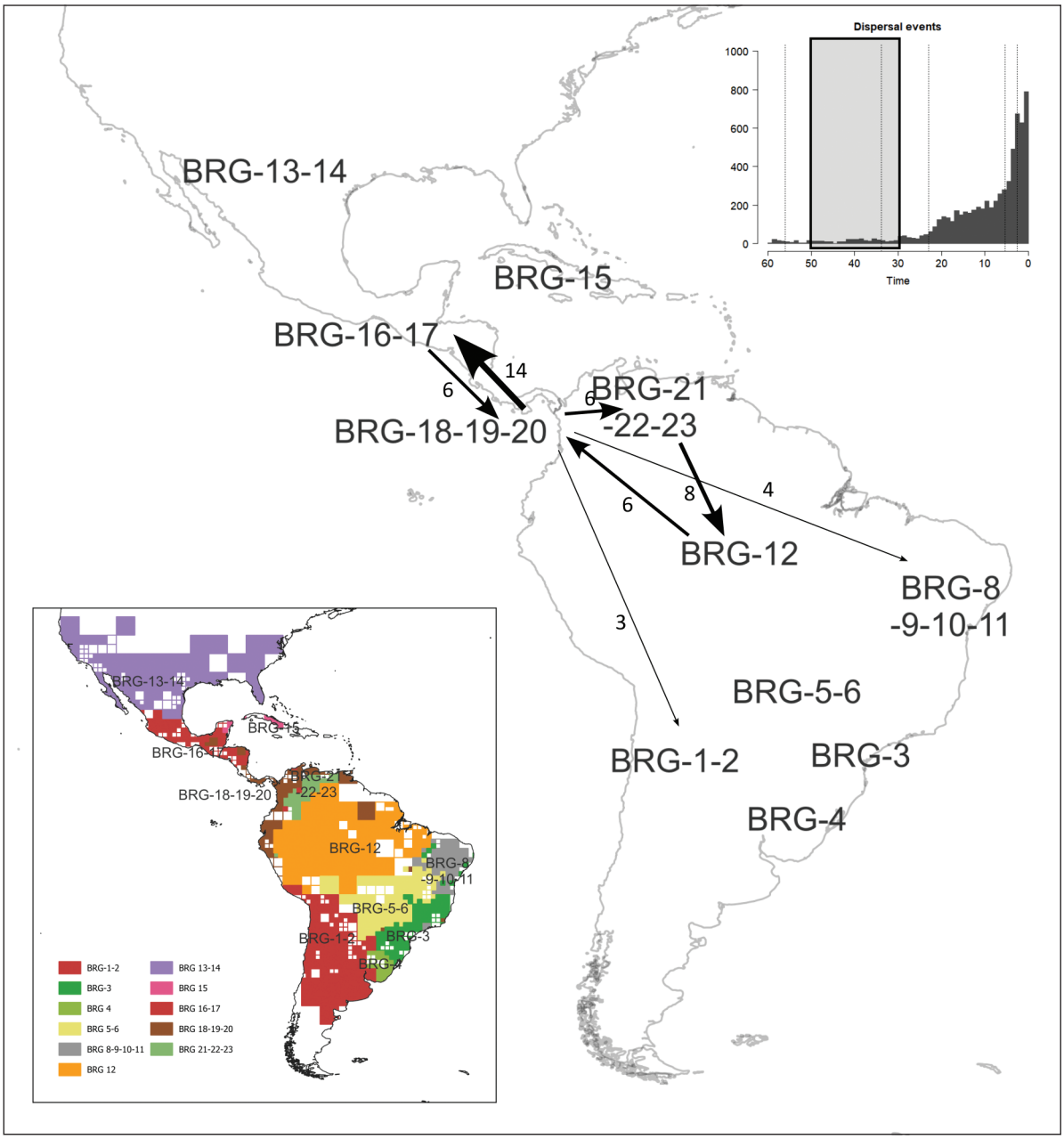

Figure 5. Most frequent dispersal routes of Triatominae between 50 and 30 Ma (phase B). Arrows represent the direction, and line thickness represents the frequency of dispersal events. The bioregion code used here represents the grouping of the original bioregions (Ferrari et al. 2022).

dispersal patterns across the Neotropics. Our findings offer novel insights into the anagenetic dispersal processes that shaped both historic and contemporary distribution of Triatominae species throughout the Americas. Specifically, we identified three distinct phases of dispersal activity during the macroevolution of the group, however, the notable decline in dispersal rates of Triatominae lineages between 50 and 30 million years ago remains an enigma.

Our time-calibrated phylogeny, constructed from the comprehensive dataset from Kieran et al. (2021) and calibrated by fossil evidence from Dominican amber, offers updated age estimates for the Triatominae subfamily. We estimate the origin of Triatominae *sensu* Masonick et al. (2025) at approximately 70.6 Ma, and the most recent common ancestor of the Triatomini, Cavernicolini, and Rhodniini tribes at 59.2 Ma. These estimates align broadly with previous molecular dating studies (e.g., Justi et al. 2016; Monteiro et al. 2018), which proposed a subfamily origin around 45 to 30 Mya. Notably, our older age estimates, especially for deeper phylogenetic nodes, suggest that the initial diversification of Triatominae likely began significantly earlier than previously recognized, potentially preceding the Andean uplift (Hoorn et al. 2010).

The biogeographic analysis of Triatominae was underpinned by the use of accurate and comprehensive distributional data. Our study drew on a robust dataset comprising a substantial dataset of 18,437 occurrence records for 96 Triatomine species obtained from the DataTri

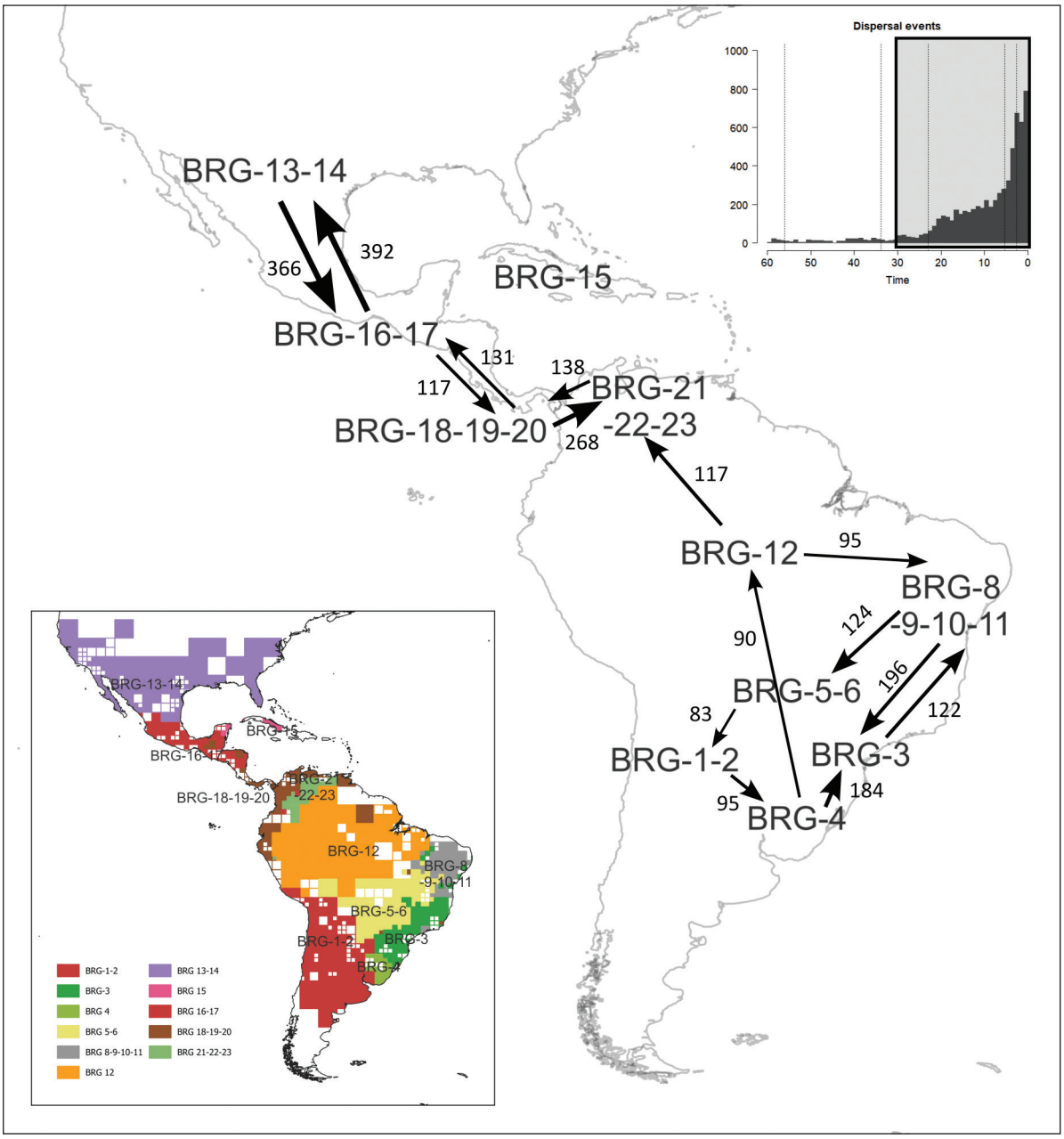

Figure 6. Most frequent dispersal routes of Triatominae between 30 and 0 Ma (phase C). Arrows represent the direction, and line thickness represents the frequency of dispersal events. The bioregion code used here represents the grouping of the original bioregions (Ferrari et al. 2022).

Database, providing a reliable basis for reconstructing historical range shifts. To examine dispersal patterns within a spatially explicit context, we employed a modified regionalization scheme comprising 11 bioregions. This framework, which visually resembles Neotropical subregions, offered a taxonomic-oriented regionalization of the study area (Ferrari et al. 2022). Notably, the regionalization revealed that a substantial proportion of species (54%) were restricted to a single bioregion (Suppl. material 1: fig. S1).

The application of the dispersal-extinction-cladogenesis (DEC) model enabled us to infer the probable geographic ranges of ancestral Triatominae lineages. Our findings suggest that the origin of the clade likely encompassed multiple areas, pointing to a widespread or complex ancestral distribution rather than a singular, narrowly defined origin. This pattern contrasts with more classical scenarios that posit a restricted point of origin followed by subsequent dispersal events (e.g. Löwenberg-Neto 2024). Nevertheless, the hypothesis that the Triatominae originated in Central and northern South America (Justi et al. 2016) remains the most plausible. The simplified DEC result (Fig. 2) highlighted BRG-18-19-20 bioregion as the most probable ancestral area, albeit with small probabilities (Suppl. material 1: fig. S2), and identified it as the richest in species diversity (cf. Diniz-Filho et al. 2013).

Analyzing the temporal dynamics of lineage dispersal provided crucial insights into the timing and intensity of biogeographic shifts. Our assessment of 100 biogeographic

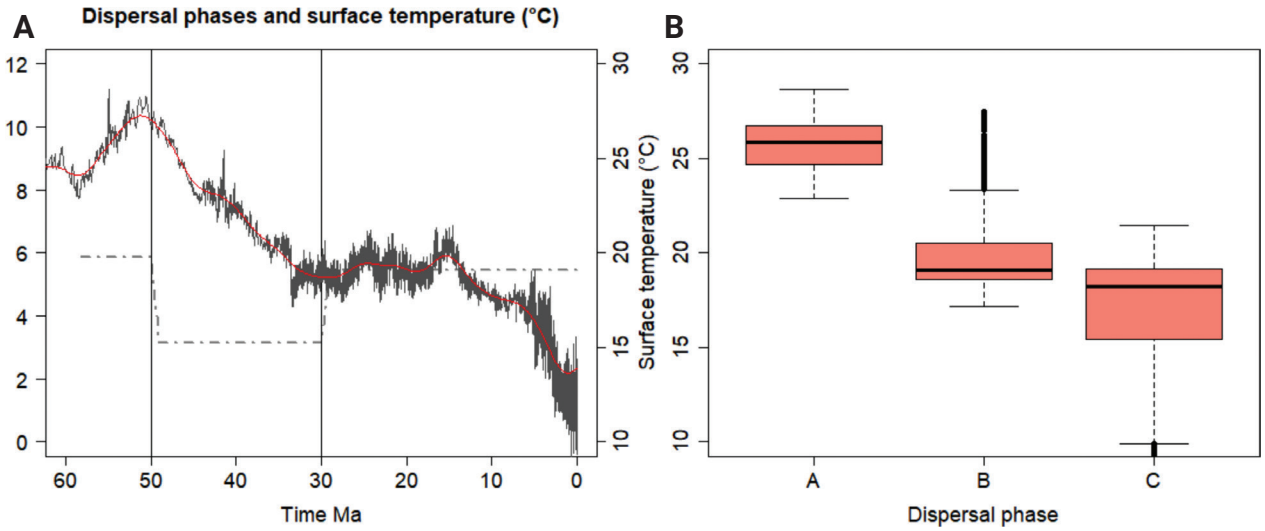

Figure 7. Triatominae dispersal phases and global paleotemperatures. **A.** Threshold regression model (dash-dotted line) and two breaking points (50 and 30 Ma, vertical solid lines); secondary y-axis: surface paleotemperatures through time (Tierney et al. 2020) and its smoothed curve (red line). **B.** Box plot of surface temperatures grouped by dispersal phase. Phase A: 60–50 Ma; phase B: 50–30 Ma; phase C: 30–0 Ma. The surface temperature distributions differed significantly among the dispersal phases.

stochastic mappings revealed distinct temporal patterns in dispersal events. Between 60 and 20 million years ago, the absolute frequency of dispersal events remained relatively low, followed by a gradual increase from 20 Ma onwards and culminating in a pronounced surge over the past 10 million years. This recent rise in absolute dispersal frequency likely reflects the growing pool of lineages available to disperse over time, as illustrated by the lineage-through-time plot. However, when dispersal rates were normalized by the number of lineages a different and arguably more informative pattern emerged. While the total number of dispersal events increased with lineage accumulation, the normalized dispersal rate was highest during the earliest phases, declined substantially thereafter, and began to rise again only gradually. This biphasic trend was further supported by the threshold regression model, which identified two significant breakpoints at 50 Ma and 30 Ma, indicating shifts in the underlying dynamics of dispersal over evolutionary time.

Examining the directionality of the most frequent dispersal routes within each identified phase allows us to reconstruct the historical movements of Triatominae lineages across the Neotropics. During Phase A (60–50 Ma), the dominant dispersal patterns involved movements from the Amazonian region towards northern South America and Mesoamerica, as well as from the Caatinga towards the Cerrado. This early phase, characterized by relatively high normalized dispersal, suggests that Amazonia may have served as an important source area for the initial expansion of Triatominae lineages into adjacent regions. These patterns occurred during a period broadly corresponding to the Paleocene-Eocene transition, a time of significant global warming (Zachos et al. 2001; Jaramillo and Cárdenas 2013), which may have influenced habitat connectivity and suitability for dispersal.

Phase B (50–30 Ma) showed a shift in dispersal dynamics, coinciding with the period of reduced normalized dispersal activity. During this phase, dispersal primarily occurred among Mesoamerica and northern South America bioregions and from Mesoamerica into the Páramos, Caatinga, and Chaco. Additionally, routes from the Páramos to Amazonia and from Amazonia to Mesoamerica were documented. The increased activity centered around Central America during this phase, despite the overall lower rate, might reflect regional diversification and limited long-distance dispersal compared to Phase A. This period spans the Eocene and Oligocene epochs, marked by climatic cooling and significant geological changes, including continued Andean uplift (Gregory-Wodzicki 2000; Hoorn et al. 2010) and sea-level fluctuations (Iturralde-Vinent and MacPhee 1999), which could have acted as barriers or filters to dispersal.

Phase C (30–0 Ma), corresponding to the resurgence in normalized dispersal rate, exhibits the most complex and frequent dispersal patterns. A high frequency of bidirectional dispersals was observed between Mesoamerica and the Nearctic region, likely facilitated by the formation and stabilization of the Isthmus of Panama (Montes et al. 2015). Dispersal events also intensified within Nearctic and Central American bioregions and between Mesoamerica and northern South America, suggesting increased connectivity and exchange. From the Amazonian region, routes extended towards northern South America and the Caatinga, indicating continued influence of Amazonia as a source or transit area (Antonelli et al. 2018). Within the Atlantic biomes, a dynamic and reciprocal exchange between the Caatinga and the Atlantic Forest was evident. Furthermore, dispersal routes following the South American dry diagonal (Caatinga -> Cerrado -> Chaco -> Pampas) highlight the importance of these drier biomes as corridors for dispersal (Simon et al. 2009; Luebert 2021). Finally, routes from the Pampas towards both the Atlantic Forest and the Amazon Forest suggest more recent expansions into these areas.

This phase encompasses the Miocene, Pliocene, and Pleistocene epochs, characterized by significant climatic oscillations, including glacial cycles, and ongoing geological processes that shaped the modern Neotropical landscape (Hoorn et al. 2010; Quattrocchio et al. 2011).

The exploratory comparison between the dispersal phases and the global surface paleotemperature record (Tierney et al. 2020) revealed a possible association between climate fluctuations and Triatominae dispersal dynamics. Phase A (60–50 Ma) corresponded with a period of relatively warmer global temperatures, including the Paleocene-Eocene Thermal Maximum. The higher dispersal rate observed during this phase might be linked to these warmer conditions, which could have facilitated the expansion of ranges and establishment in new areas, particularly from tropical source regions like Amazonia. Phase B (50–30 Ma) aligned with a period of global cooling, including the transition into the Oligocene, which saw a significant drop in global temperatures. Previous analyses of global plant range shifts revealed an approximately 30% decrease in movements into the world's tropics during the Early Eocene Climatic Optimum around 52 Ma (Antonelli et al. 2015), suggesting large-scale, albeit poorly understood, vegetational changes influencing dispersal dynamics during this warm interval. For the Triatominae lineages, the observed decline and stabilization in the dispersal rate during this phase could be a direct consequence of this cooling trend. Cooler temperatures might have reduced habitat suitability, increased environmental filtering, or restricted connectivity between regions, thereby limiting dispersal success (Garcia et al. 2014). Phase C (30–0 Ma) encompasses a period of fluctuating but generally recovering temperatures compared to the Oligocene minimum, leading into the more recent Quaternary glacial cycles. The resurgence in dispersal activity during this phase suggested that conditions became more favorable again (Antonelli et al. 2015). While this period includes significant climatic variability, the overall trend allowed for increased movement and establishment, potentially driven by the expansion and contraction of biomes in response to climate shifts, creating new opportunities for dispersal and colonization.

A closer examination of the temporal distribution of the topmost frequent dispersal routes provides finer-scale insights into the timing of specific biogeographic connections. While the overall normalized rate shows broad phases, individual routes exhibit varying temporal peaks and durations of activity (Suppl. material 1: fig. S3, table S2). For instance, the bidirectional exchange between Mesoamerica (BRG-16-17) and Nearctic region (BRG-13-14) showed distinct modes of activity, with one mode peaking earlier (around 13–15 Ma) and another being more recent. Similarly, routes originating from northern South America (BRG-18-19-20) showed activity spanning from the early phases to more recent times, but with different temporal distributions depending on the target region (e.g., dispersal to BRG-21-22-23 vs. BRG-16-17).

In summary, our study provided a comprehensive temporal and spatial reconstruction of Triatominae lineage dispersals across the Neotropics. Rather than providing detailed historical narratives for each clade or species group, we offer the first comprehensive overview of dispersal routes undertaken by Triatominae lineages during their evolution in the Americas. The biphasic pattern of rate of dispersal activity highlighted periods of both reduced and increased movement. The association between dispersal phases and paleotemperatures, while exploratory, suggested that the observed shifts in dispersal dynamics were associated with significant variations in paleotemperature, implying a potential influence of climatic shifts on the evolutionary dispersal processes.

Acknowledgements

Analyses were run at the Ecoevol-cluster (LETS-UFG/BR). We thank A. Ferrari (FURG/BR) for sharing the bioregions shapefiles. We are grateful to F. C. V. Zanella (UNILA/BR), L. R. R. Faria-Junior (UNILA/BR), M. Pie (UFPR/BR), J. J. Morrone (UNAM/MX), A. Ferrari (FURG/BR), A. S. de Paula (UFOP/BR), and I. L. F. Magalhães (MACN/AR) for their comments on earlier version of the manuscript. We would like to thank UNILA/BR for granting support for our research activities (PRPPG 121/2023 - PAAP). This research was supported by *Coordenação de Aperfeiçoamento de Pessoal de Nível Superior* - Brazil (CAPES).

Author contributions

MBC: Conceptualization, methodology, investigation, formal analysis, data curation, writing-original, writing-review and editing. JER: Conceptualization, investigation, writing-review and editing, supervision. AL: Data curation, methodology, formal analysis, writing-review and editing. PLN: Conceptualization, methodology, investigation, formal analysis, writing-original, visualization, writing-review and editing, supervision, project administration.

Data accessibility statement

The phylogenetic tree used as input in MD-Cat is available from Kieran et al. (2021), and the dated tree are available at Zenodo under doi: https://doi.org/10.5281/zenodo.15585954 (accessible link: https://zenodo.org/uploads/15585954?token=eyJhbGciOiJIUzUxMiJ9.eyJpZCI6IjExY2Q1NjJhLTVjY2UtNDQ2NC1hMWFkLTI5MDE4YmVlMmE5NyIsImRhdGEiOnt9LCJyYW5kb20iOiIwYmI5NmNhOWI5MzQxOTRiYmExMDliYjE2OWU5OWM2MCJ9.YcWDZmjhcWbS04pSmL9YG44WLfQ2AX5cTgh0VS9cftPNjaL0CI-rMaKyzNwtItrshfBLNbtPeanSkFeuDsOVrQ). Species occurrences were available in the DataTRI dataset (Ceccarelli et al. 2022), and shapefiles of the bioregions were obtained from Ferrari et al. (2022).

References

Abad-Franch F, Monteiro FA (2007) Biogeography and evolution of Amazonian triatomines (Heteroptera: Reduviidae): implications for Chagas disease surveillance in humid forest ecoregions. Memórias do Instituto Oswaldo Cruz 102(sup. 1): 57–69. https://doi.org/10.1590/s0074-02762007005000108

Abad-Franch F, Monteiro F, Jaramillo N, Gurgel-Gonçalves R, Dias F, Diotaiuti L (2009) Ecology, evolution, and the long-term surveillance of vector-borne Chagas disease: a multi-scale appraisal of the tribe Rhodniini (Triatominae). Acta Tropica 110: 159–177. https://doi.org/10.1016/j.actatropica.2008.06.005

Alevi K, Oliveira J, Silva Rocha D, Galvão C (2021) Trends in taxonomy of Chagas disease vectors (Hemiptera, Reduviidae, Triatominae): From Linnaean to integrative taxonomy. Pathogens 10: 1627. https://doi.org/10.3390/pathogens10121627

Antonelli A, Zizka A, Silvestro D, Scharn R, Cascales-Miñana B, Bacon C (2015) An engine for global plant diversity: highest evolutionary turnover and emigration in the American tropics. Frontiers in Genetics 6: 130. https://doi.org/10.3389/fgene.2015.00130

Antonelli A, Zizka A, Carvalho F, Scharn R, Bacon C, Silvestro D, Condamine F (2018) Amazonia is the primary source of Neotropical biodiversity. Proceedings of the National Academy of Sciences of the United States of America 115: 6034–6039. https://doi.org/10.1073/pnas.1713819115

Bargues MD, Klisiowicz DR, Panzera F, Noireau F, Marcilla A, Perez R, Rojas MG, O'Connor JE, Gonzalez-Candelas F, Galvão C, Jurberg J, Carcavallo RU, Dujardin JP, Mas-Coma S (2006) Origin and phylogeography of the Chagas disease main vector *Triatoma infestans* based on nuclear rDNA sequences and genome size. Infection, Genetics and Evolution 6: 46–62. https://doi.org/10.1016/j.meegid.2005.01.006

Ceccarelli S, Justi SA, Rabinovich JE, Diniz-Filho JAF, Villalobos F (2020) Phylogenetic structure of geographical co-occurrence among New World Triatominae species, vectors of Chagas disease. Journal of Biogeography 47: 1218–1231. https://doi.org/10.1111/jbi.13810

Ceccarelli S, Balsalobre A, Vicente ME, Curtis-Roble R, Hamer SA, Landa JMA, Rabinovich JE, Marti GA (2022) American triatomine species occurrences: updates and novelties in the DataTri database. GigaByte, 1–14. https://doi.org/10.46471/gigabyte.62

Diniz-Filho JAF, Ceccarelli S, Hasperué W, Rabinovich J (2013) Geographical patterns of Triatominae (Heteroptera: Reduviidae) richness and distribution in the Western Hemisphere. Insect Conservation and Diversity 6: 704–714. https://doi.org/10.1111/icad.12025

Dornelas M, Magurran A, Buckland S, Chao A, Chazdon RL, Colwell RK, Curtis T, Gaston KJ, Gotelli J, Kosnik MA, Mcgill B, Mccune JL, Morlon H, Mumby PJ, Ovreas L, Studeny A, Vellend M (2013) Quantifying temporal change in biodiversity: challenges and opportunities. Proceedings of the Royal Society B: Biological Sciences 280: 20121931. https://doi.org/10.1098/rspb.2012.1931

Dupin J, Matzke NJ, Särkinen T, Knapp S, Olmstead RG, Bohs L, Smith SD (2017) Bayesian estimation of the global biogeographical history of the Solanaceae. Journal of Biogeography 44: 887–899. https://doi.org/10.1111/jbi.12898

Edler D, Guedes T, Zizka A, Rosvall M, Antonelli A (2017) Infomap bioregions: Interactive mapping of biogeographical regions from species distributions. Systematic Biology 66: 197–204. https://doi.org/10.1093/sysbio/syw087

Else JG, Cheong WH, Mahadevan S, Zárate LG (1977) A new species of cave-inhabiting *Triatoma* (Hemiptera: Reduviidae) from Malaysia. Journal of Medical Entomology 14: 367–369. https://doi.org/10.1093/jmedent/14.3.367

Fergnani P, Ruggiero A, Ceccarelli S, Menu F, Rabinovich J (2013) Large-scale patterns in morphological diversity and species assemblages in Neotropical Triatominae (Heteroptera: Reduviidae). Memorias do Instituto Oswaldo Cruz 108: 997–1008. https://doi.org/10.1590/0074-0276130369

Ferrari A, Janisch-Alvares D, Buratto P, Ribeiro-Barao K (2022) Distribution patterns of Triatominae (Hemiptera: Reduviidae) in the Americas: an analysis based on networks and endemicity. Cladistics 38: 563–581. https://doi.org/10.1111/cla.12500

Forattini O, da Rocha e Silva E, Ferreira O, Rabello E, Ferreira Santos J, Ribeiro de Lima A (1977) Aspectos ecológicos da Tripanossomiase americana. XI. Domiciliação de *Panstrongylus megistus* e potencial enzoótico. Revista de Saúde Pública 11: 527–550. https://doi.org/10.1590/S0034-89101977000400010

Galvão C, Justi SA (2015) An overview on the ecology of Triatominae (Hemiptera: Reduviidae). Acta Tropica 151: 116–125. https://doi.org/10.1016/j.actatropica.2015.06.006

Galvão C, Patterson JS, Rocha DS, Jurberg J (2002) A checklist of the Triatominae (Hemiptera: Reduviidae). In: Galvão C, Carcavallo RU, Rocha DS, Jurberg J (Eds) Atlas dos vetores da doença de Chagas nas Américas, volume II. Editora Fiocruz, Rio de Janeiro.

Garcia RA, Cabeza M, Rahbek C, Araújo MB (2014) Multiple dimensions of climate change and their implications for biodiversity. Science 344(6183): 1247579. https://doi.org/10.1126/science.1247579

Ghauri MSK (1976) The Indian triatomine genus *Linshcosteus* (Reduviidae). Systematic Entomology 1: 183–187. https://doi.org/10.1111/j.1365-3113.1976.tb00037.x

Gregory-Wodzicki K (2000) Uplift history of the central and northern Andes: a review. Geological Society of America Bulletin 112: 1091–1105. https://doi.org/10.1130/0016-7606(2000)112%3C1091:UHOTCA%3E2.3.CO;2

Gürtler RE, Ceballos LA, Ordoñez-Krasnowski P, Lanati LA, Stariolo R, Kitron U (2009) Strong host-feeding preferences of the vector *Triatoma infestans* modified by vector density: implications for the epidemiology of Chagas disease. PLoS Neglected Tropical Diseases 3: e447. https://doi.org/10.1371/journal.pntd.0000447

Hackel J, Sanmartín I (2021) Modelling the tempo and mode of lineage dispersal. Trends in Ecology & Evolution 36: 1102–1112. https://doi.org/10.1016/j.tree.2021.07.007

Hansen J, Sato M, Russell G, Kharecha P (2013) Climate sensitivity, sea level and atmospheric carbon dioxide. Philosophical Transactions of the Royal Society A: Mathematical, Physical and Engineering Sciences 371: 2001. https://doi.org/10.1098/rsta.2012.0294

Hoorn C, Wesselingh F, Ter Steege H, Bermudez MA, Mora A, Sevink J, Sanmartín I, Sanchez-Meseguer A, Anderson CL, Figueiredo JP, Jaramillo C, Riff D, Negri FR, Hooghiemstra H, Lundberg J, Stadler T, Särkinen T, Antonelli A (2010) Amazonia through time: Andean uplift, climate change, landscape evolution, and biodiversity. Science 330: 927–931. https://doi.org/10.1126/science.1194585

Hwang WS, Weirauch C (2012) Evolutionary history of assassin bugs (Insecta: Hemiptera: Reduviidae): insights from divergence dating

and ancestral state reconstruction. PLoS ONE 7: e45523. https://doi.org/10.1371/journal.pone.0045523

Ibarra-Cerdeña C, Zaldívar-Riverón A, Peterson A, Sánchez-Cordero V, Ramsey JM (2014) Phylogeny and niche conservatism in North and Central American Triatomine bugs (Hemiptera: Reduviidae: Triatominae), vectors of Chagas disease. PLoS Neglected Tropical Diseases 8: e3266. https://doi.org/10.1371/journal.pntd.0003266

Iturralde-Vinent M, Macphee R (1999) Paleogeography of the Caribbean region: implications for Cenozoic biogeography. Bulletin of the American Museum of Natural History 238: 1–95.

Iturralde-Vinent MA, MacPhee RD (2019) Remarks on the age of Dominican amber. Palaeoentomology 2: 236–240. https://doi.org/10.11646/palaeoentomology.2.3.7

Jaramillo C, Cárdenas A (2013) Global warming and neotropical rainforests: a historical perspective. Annual Review of Earth and Planetary Sciences 41: 741–766. https://doi.org/10.1146/annurev-earth-042711-105403

Justi S, Galvão C (2017) The evolutionary origin of diversity in Chagas disease vectors. Trends in Parasitology 33: 42–52. https://doi.org/10.1016/j.pt.2016.11.002

Justi S, Galvão C, Schrago C (2016) Geological changes of the Americas and their influence on the diversification of the Neotropical kissing bugs (Hemiptera: Reduviidae: Triatominae). PLoS Neglected Tropical Diseases 10: e0004527. https://doi.org/10.1371/journal.pntd.000452

Kieran TJ, Gordon ER, Zaldívar-Riverón A, Ibarra-Cerdeña CN, Glenn TC, Weirauch C (2021) Ultraconserved elements reconstruct the evolution of Chagas disease-vectoring kissing bugs (Reduviidae: Triatominae). Systematic Entomology 46: 725–740. https://doi.org/10.1111/syen.12485

Knyshov A, Gordon ER, Masonick PK, Castillo S, Forero D, Hoey-Chamberlain R, Hwang WS, Johnson KP, Lemmon AR, Moriarty Lemmon E, Standring S, Zhang J Weirauch C (2023) Chromosome-aware phylogenomics of assassin bugs (Hemiptera: Reduvioidea) elucidates ancient gene conflict. Molecular Biology and Evolution 40: msad168. https://doi.org/10.1093/molbev/msad168

Leite GR (2013) Biogeografia do gênero *Triatoma* Laporte, 1832 (Hemiptera, Reduviidae, Triatominae): distribuição, padrões de riqueza, endemismo e diversificação. PhD Thesis, Universidade Federal do Espírito Santo, Brazil.

Löwenberg-Neto P (2024) Validating the timing of New World monkey dispersal routes by lineage dispersal modeling and description of the Amazonian eastward route. Journal of Mammalian Evolution 31: 1–14. https://doi.org/10.1007/s10914-024-09714-7

Löwenberg-Neto P, De Carvalho C (2020) Neotropical endemism and dispersal events between tropical and extra-tropical regions underlay the reticulate assemblages of muscid flies. Journal of Biogeography 47: 1574–1584. https://doi.org/10.1111/jbi.13835

Luebert F (2021) The two South American dry diagonals. Frontiers of Biogeography, 13: 1–14. https://doi.org/10.21425/F5FBG51267

Magalhaes ILF, Santos AJ, Ramírez MJ (2021) Incorporating topological and age uncertainty into event-based biogeography of sand spiders supports paleo-islands in Galapagos and ancient connections among neotropical dry forests. Diversity 13:1–23. https://doi.org/10.3390/d13090418

Mai U, Charvel E, Mirarab S (2024) Expectation-Maximization enables phylogenetic dating under a categorical rate model. Systematic Biology 73: 823–838. https://doi.org/10.1093/sysbio/syae034

Masonick PK, Knyshov A, Gordon ER, Forero D, Hwang WS, Hoey-Chamberlain R, Bush T, Castillo S, Hernandez M, Ramirez J, Standring S, Zhang J, Weirauch, C. (2025) A revised classification of the assassin bugs (Hemiptera: Heteroptera: Reduviidae) based on combined analysis of phylogenomic and morphological data. Systematic Entomology 50: 102–138. https://doi.org/10.1111/syen.12646

Matzke NJ (2018). BioGeoBEARS: BioGeography with Bayesian (and likelihood) Evolutionary Analysis with R Scripts. version 1.1.1, published on GitHub on November 6, 2018. https://doi.org/10.5281/zenodo.1478250

Minter D (1976) Feeding patterns of some Triatomine vector species. In: Pan American Health Organization (Ed) New approaches in American Trypanosomiasis research. Proceedings of an international symposium, Scientific Publications, Belo Horizonte, 34–37.

Monteiro F, Weirauch C, Felix M, Lazoski C, Abad-Franch F (2018) Evolution, systematics, and biogeography of the Triatominae, vectors of Chagas disease. Advances in Parasitology 99: 265–344. https://doi.org/10.1016/bs.apar.2017.12.002

Montes C, Cardona A, Jaramillo C, Pardo A, Silva JC, Valencia V, Ayala C, Pérez-Ángel LC, Rodríguez-Parra LA, Ramírez V, Niño H (2015) Middle Miocene closure of the Central American Seaway. Science 348(6231): 226–229. https://doi.org/10.1126/science.aaa2815

Noguchi K, Gel Y, Duguay C (2011) Bootstrap-based tests for trends in hydrological time series, with application to ice phenology data. Journal of Hydrology 410: 150–161. https://doi.org/10.1016/j.jhydrol.2011.09.008

Noireau F, Dujardin J (2010) Biology of Triatominae. In: Tibayrenc M, Telleria J (Eds) American Trypanosomiasis Chagas disease: One hundred years of research. Elsevier international, 149–168. https://doi.org/10.1016/B978-0-12-384876-5.00007-1

Paradis E, Schliep K (2019) Ape 5.0: An environment for modern phylogenetics and evolutionary analyses in R. Bioinformatics 35: 526–528. https://doi.org/10.1093/bioinformatics/bty633

Poinar-Jr G (2005) *Triatoma dominicana* sp. n. (Hemiptera: Reduviidae: Triatominae), and *Trypanosoma antiquus* sp. n. (Stercoraria: Trypanosomatidae), the first fossil evidence of a Triatomine-Trypanosomatid vector association. Vector-Borne and Zoonotic Diseases 5: 72–81. https://doi.org/10.1089/vbz.2005.5.7

Poinar-Jr G (2013) *Panstrongylus hispaniolae* sp. n. (Hemiptera: Reduviidae: Triatominae), a new fossil triatomine in Dominican amber, with evidence of gut flagellates. Palaeodiversity 6: 1–8.

Poinar-Jr G (2019) A primitive triatomine bug, *Paleotriatoma metaxytaxa* gen. et sp. nov. (Hemiptera: Reduviidae: Triatominae), in mid-Cretaceous amber from northern Myanmar. Cretaceous Research 93: 90–97. https://doi.org/10.1016/j.cretres.2018.09.004

Paula A, Barreto C, Telmo M, Diotaiuti L, Galvão C (2021) Historical biogeography and the evolution of hematophagy in Rhodniini (Heteroptera: Reduviidae: Triatominae). Frontiers in Ecology and Evolution 9: 1–13. https://doi.org/10.3389/fevo.2021.660151

Quattrocchio M, Volkheimer W, Borromei A, Martinez M (2011) Changes of the palynobiotas in the Mesozoic and Cenozoic of Patagonia: a review. Biological Journal of the Linnean Society 103: 380–396. https://doi.org/10.1111/j.1095-8312.2011.01652.x

Rabinovich JE, Kitron U, Obed Y, Yoshioka M, Gottdenker N, Chaves L (2011) Ecological patterns of blood-feeding by kissing-bugs (Hemiptera: Reduviidae: Triatominae). Memórias Do Instituto Oswaldo Cruz 106: 479–494. https://doi.org/10.1590/S0074-02762011000400016

Ree R, Moore B (2005) A likelihood framework for inferring the evolution of geographic range on phylogenetic trees. Evolution 59: 2299–2311. https://doi.org/10.1111/j.0014-3820.2005.tb00940.x

Ree R, Smith S (2008) Maximum likelihood inference of geographic range evolution by dispersal, local extinction, and cladogenesis. Systematic Biology 57: 4–14. https://doi.org/10.1080/10635150701883881

Ree R, Sanmartín I (2018) Conceptual and statistical problems with the DEC+J model of founder-event speciation and its comparison with DEC via model selection. Journal of Biogeography 45: 741–749. https://doi.org/10.1111/jbi.13173

Rodriguero M, Gorla D (2004) Latitudinal gradient in species richness of the New World Triatominae (Reduviidae). Global Ecology and Biogeography 13: 75–84. https://doi.org/10.1111/j.1466-882X.2004.00071.x

Simon M, Grether R, de Queiroz L, Skema C, Pennington T, Hughes C (2009) Recent assembly of the Cerrado, a Neotropical plant diversity hotspot, by in situ evolution of adaptations to fire. The Proceedings of the National Academy of Sciences 106: 20359–20364. https://doi.org/10.1073/pnas.0903410106

Stamatakis A (2014) RAxML version 8: a tool for phylogenetic analysis and post-analysis of large phylogenies. Bioinformatics 30: 1312–1313. https://doi.org/10.1093/bioinformatics/btu033

Weirauch C (2021). Origin and evolution of Triatominae. In: Guarneri A, Lorenzo M (Eds) Triatominae - The Biology of Chagas Disease Vectors, Entomology in Focus, 5 Springer Nature, 1–13. https://doi.org/10.1007/978-3-030-64548-9_1

Zachos J, Pagani M, Sloan L, Thomas E, Billups K (2001) Trends, rhythms, and aberrations in global climate 65 Ma to present. Science 292: 686–693. https://doi.org/10.1126/science.1059412

Zeileis A, Leisch F, Hornik K, Kleiber C (2002) strucchange: An R Package for testing for structural change in linear regression models. Journal of Statistical Software 7:1–38. https://doi.org/10.18637/jss.v007.i02

Zhang J, Gordon ER, Forthman M, Hwang WS, Walden K, Swanson DR, Kevin JP, Rudolf M, Weirauch C (2016) Evolution of the assassin's arms: insights from a phylogeny of combined transcriptomic and ribosomal DNA data (Heteroptera: Reduvioidea). Scientific Reports 6: 22177. https://doi.org/10.1038/srep22177

Supplementary materials

Supplementary material 1

Additional tables and figures (.docx)

Link: https://doi.org/10.21425/fob.18.132274.suppl1